Synthetic approaches to the preparation of hybrid network materials incorporating carborane clusters

Arántzazu González-Campo,†[a] Rosario Núñez,*[a] Clara Viñas[a] and Bruno Boury[b]

Received (in Montpellier, France) 24th November 2005, Accepted 23rd February 2006
First published as an Advance Article on the web 8th March 2006
DOI: 10.1039/b516705c

A novel type of hybrid organic–inorganic class II materials with carborane-containing units have been prepared from a particular trichlorosilylcarborane-containing precursor. Different polymerisation processes were investigated in order to achieve the formation of materials that incorporate the covalently bonded carborane units and exhibit different structural characteristics. Hydrolytic, and non-hydrolytic sol–gel process were used for the preparation of the hybrid materials with an Si–O–Si-based network, whereas the hybrid material with an Si–N═C═N–Si-based network was prepared by a carbodiimide sol–gel process. Structural characterisation was performed by solid state NMR, IR, porosimetry and X-ray powder diffraction that reveal the formation of non-porous to porous materials with a high level of polycondensation, a short-range order organisation and the preservation of the covalent bond between the carborane part and the inorganic network. Alternatively, a solid-state process was used and allows the preparation of materials with a higher level of organisation according to polarized light microscopy. The materials are stable to about 450 °C in inert atmosphere, suggesting good thermal stability.

Introduction

The *closo*-1,2-carborane and its derivatives combine, in a unique three-dimensional symmetrical rigid cluster-like structure, high stability (chemical, photochemical and thermal) with a highly polarizable σ-aromatic character.[1–6] All this make these clusters good candidates for non-linear optical materials;[7–9] liquid crystals with specific mesophase, birefringence and photochemical stability;[10–14] or organic–inorganic hybrid carborane–siloxane polymers and preceramic precursors that exhibit outstanding thermal and oxidative properties.[15–19] In addition, carboranes have been used to prepare a great variety of coordination compounds and have been suitable for a wide range of applications such as catalysis,[20–26] radiopharmaceuticals,[27,28] and conducting organic polymers,[29] among others.[30–32]

The carborane cluster could represent an attractive versatile group for the preparation of organic–inorganic hybrid materials due to its intrinsic properties. We found interesting to synthesize some of them that could be seen as models for a subsequent development of carborane-containing hybrid materials. Nowadays, there is significant interest in materials that combine in a hybrid material high dimensional, thermal and oxidative stability.[33] Among them, the *bridged polysilsesquioxanes* are functional organic–inorganic materials prepared by a sol–gel process,[34,35] with the ideal chemical formula R–[$SiO_{1.5}$]$_n$,[33,36–38] which combine the properties of the organic and inorganic parts. In this respect, the organic bridging group attached to the Si atoms can be very different in terms of length, rigidity and functionality, which provides the chance to modulate properties such as porosity, thermal stability, and chemical reactivity, among others. Likewise, the control of porosity, thermomechanical properties and short to long-range order organisation have been some of the main purposes in the selection of an organic spacer.[39]

Thus, we report here an approach to the preparation and characterization of hybrid materials, where the "organo-functional" part contains a carborane moiety. In this respect, we study the preparation of carborane–organo-poly(trichlorosilyl), R–[$Si(Cl)_3$]$_2$ (R = carborane–organic part), in order to work with the trichlorosilyl-polymerizable group,[40] which allows the formation of hybrid materials by either hydrolytic or non-hydrolytic sol–gel processes. Additionally, we compare the solvent processes with a solid-state process that leads to more periodically organised materials.[41] This type of trichlorosilyl precursor was recently demonstrated to be useful for the preparation of silsesquicarbodiimide, a type of hybrid material containing Si–N═C═N–Si linkages.[42–44] Therefore, starting with the same precursor we investigate the possibility to prepare carborane-containing silsesquioxanes by four different ways, and to characterize these solids in terms of structure, porosity, level of condensation and thermal stability.

Results and discussion

Synthesis and characterization of precursors

The preparation of the precursors relies on the weak acidity of the $C_{cluster}$–H (C_c–H) protons in carboranes (pK_a = 23.0),[45] that can be removed by strong bases generating nucleophile anions. These have the ability to react with a wide range of electrophilic reagents, such as halogens, alkyl halides,

[a] *Institut de Ciència de Materials de Barcelona CSIC, Campus UAB, E-08193 Bellaterra, Spain. E-mail: rosario@icmab.es*
[b] *Laboratoire de Chimie Moleculaire et Organisation du Solide, UMR 5637, Université de Montpellier II, Place E. Bataillon, F-34095 Montpellier Cedex 5, France*
† Enrolled in the UAB PhD program.

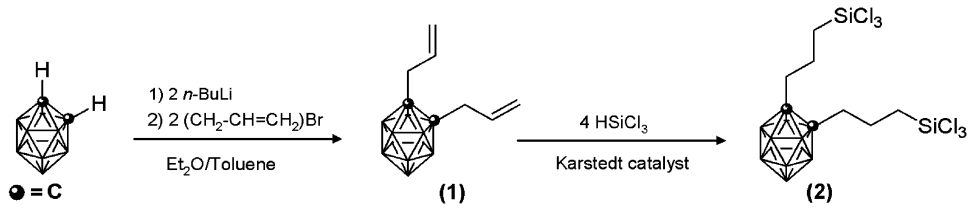

Scheme 1 Synthesis of 1,2-$(CH_2–CH{=}CH_2)_2$-1,2-$C_2B_{10}H_{10}$ (**1**) and 1,2-$((CH_2)_3SiCl_3)_2$-1,2-$C_2B_{10}H_{10}$ (**2**) from 1,2-$C_2B_{10}H_{12}$.

chlorosilanes, *etc.*[46] Thus, compound **1**, 1,2-$(CH_2–CH{=}CH_2)_2$-1,2-$C_2B_{10}H_{10}$ was prepared by the reaction of the dilithium salt of the *o*-carborane with the stoichiometric amount of allyl bromide, according to Scheme 1. The resultant yellow oil was characterized by IR, $^1H\{^{11}B\}$, $^{13}C\{^1H\}$ and ^{11}B NMR. Three resonances at 2.9, 5.2 and 5.8 ppm are observed in the $^1H\{^{11}B\}$ NMR spectrum and are attributed respectively to $C_{cluster}–CH_2$, CH and CH_2 of the allyl group. The corresponding resonances at 39.2, 132.5 and 119.5 ppm are also exhibited in the $^{13}C\{^1H\}$ NMR spectrum, whereas the peak at 77.7 ppm is assigned to the $C_{cluster}$ atoms (C_c). The ^{11}B NMR spectrum exhibits two resonances, at −4.5 and −10.6 ppm, with a 2 : 8 pattern.

The hydrosilylation reaction with $HSiCl_3$ of the allylic function bonded to the carborane moiety in **1**, for two hours at room temperature in the presence of Karstedt catalyst, gave quantitatively the trichlorosilane **2** (99% yield) (Scheme 1). Precursor **2** was obtained as a yellow oil, for which $^{29}Si\{^1H\}$ NMR analysis revealed the presence of only one signal at 11.6 ppm. Other NMR data obtained by $^1H\{^{11}B\}$ and $^{13}C\{^1H\}$ NMR indicated almost complete hydrosilylation (98%) in the β position.

Preparation of the hybrid materials

Four different methods using precursor **2** have been used: hydrolytic sol–gel, non-hydrolytic sol–gel, solid-state and carbodiimide processes.

According to a classical hydrolytic sol–gel process, xerogel **3** was prepared by hydrolysis–polycondensation using a stoichiometric amount of water dissolved in THF at room temperature (see Scheme 2). The gel was rapidly formed and allowed to age for 7 days. After washing with the corresponding solvents, the gel was dried to give an insoluble and brittle powder.

Likewise, a non-hydrolytic sol–gel process was used for the preparation of xerogel **4**, using diisopropyl ether as oxygen donor and $FeCl_3$ (0.1%) as catalyst, under argon at 110 °C for 43 hours (Scheme 2).[47,48]

The solid-state hydrolytic process was usable since chlorosilanes are highly reactive toward water,[49] and xerogel **5** was obtained by exposing the precursor **2** to the air for 19 days.

A carbodiimide sol–gel-like process based on the exchange reaction between Si–N and Si–Cl bonds was also investigated in order to prepare a Si–N=C=N–Si network different from the oxide network that results from the hydrolytic or the non-hydrolytic process. According to Scheme 2, xerogel **6** was obtained by sol–gel polycondensation of **2** with bis(trimethylsilyl)carbodiimide in THF at room temperature in the presence of pyridine as catalyst. The opaque white gel was aged for 7 days at 45 °C, washed with THF to remove by-products and pyridine, and dried under vacuum at 130 °C for 1 day to give xerogel **6**.

Characterization of the hybrid materials

Molecular structure. The IR spectra (KBr pellet) of xerogels **3**, **4** and **5** exhibit strong bands at 2594 cm^{-1} corresponding to the B–H stretching mode, which indicates the presence of the cluster in the material, and those at 1078 cm^{-1} are related to Si–O–Si stretches that indicate the condensation of the precursor Si–Cl functions. Bands at 3400 and 3600 cm^{-1}

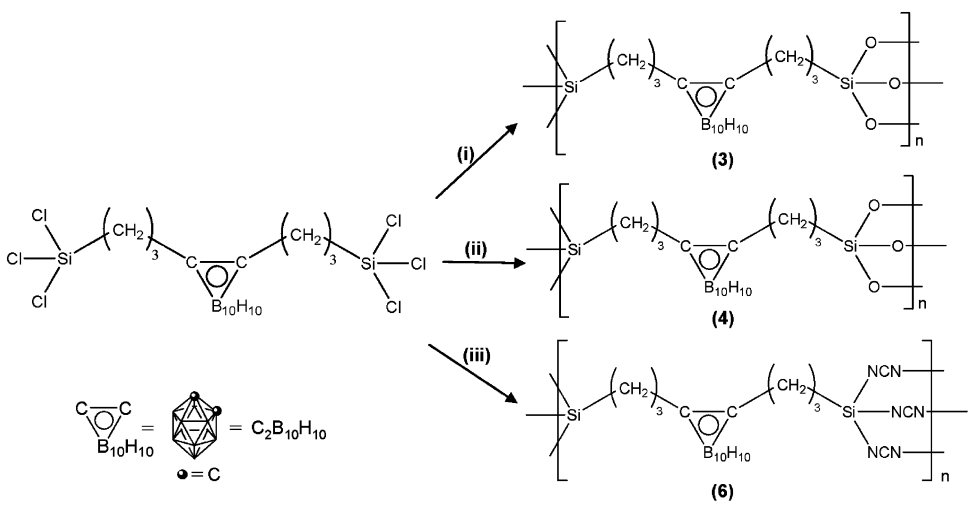

Scheme 2 Preparation of xerogels **3**, **4** and **6**; (i) H_2O, THF, (ii) $(^iPr)_2O$, $FeCl_3$, (iii) $Me_3Si–N{=}C{=}N–SiMe_3$, THF, pyridine.

corresponding to SiO–H are insignificant and the band near 1600 cm^{-1} due to H_2O is very small for xerogels **3–5**. Other bands observed in the region 2950–2880 and 1250 cm^{-1} corroborate the presence of the alkyl chain in the hybrid material. For **6**, two strong absorption bands at 2592 and 2152 cm^{-1} correspond respectively to the B–H stretching and the carbodiimide group (Si–NCN). Upon contact with moisture, hydrolysis of the Si–NCN groups occurs, with subsequent Si–O–Si polycondensation ($\nu_{Si-O-Si}$ = 1063 cm^{-1}), and cyanamide groups (ν_{N-CN} = 2265 cm^{-1}) that replace the carbodiimide units (Si–NCN).[43]

The ^{13}C CP MAS NMR spectra of xerogels **3** and **4** also confirm that the integrity of the molecular building block survives the sol–gel polymerization, and that the Si–C and C_c–C bonds cleavage does not occur. Three peaks around 14, 24 and 37 ppm corresponding to Si–CH_2–CH_2–CH_2–$C_{cluster}$ alkyl spacers are observed, while a broad peak centred at 80 ppm is attributed to the C_c atoms. For **6**, the ^{13}C CP MAS NMR spectrum exhibits peaks at 18 ppm (*C*H_2–Si), 24 ppm (*C*H_2–CH_2), 38 ppm (C_c–*C*H_2), 80 ppm (C_c) and 121 ppm (N*C*N). The chemical shifts of the bridging alkylene carbons are very similar to those observed for silica-based xerogels **3** and **4**, partially due to the similar electronegativity of the NCN function and the oxygen atoms.[42]

An evaluation of the degree of condensation of the polysiloxane network was obtained by looking at the ^{29}Si CP MAS NMR spectroscopic analyses. Both xerogels **3** and **4**, exhibit three broad peaks at δ −49, −56 and −65 ppm, corresponding to T^1 [SiC(OH)$_2$(OSi)], T^2 [SiC(OH)(OSi)$_2$] and T^3 [SiC(OSi)$_3$], respectively. No signals in the range of −100 to −110 ppm due to Q^n substructures are observed, which confirms that Si–C bonds are not cleaved during the condensation process. ^{29}Si CP MAS NMR spectroscopy can be used to evaluate quantitatively the level of condensation (LC) according to the formula LC = 1/3 T^1 + 2/3 T^2 + 1 T^3.[50] In both xerogels **3** and **4**, the LC was 75% by deconvolution of the ^{29}Si CP MAS NMR spectra (Table 1). However, xerogel **3** prepared by the hydrolytic sol–gel process shows more T^3 and T^1 substructures than xerogel **4**, which presents negligible T^1 units (6%) and major T^2 and T^3. Altogether, **4** prepared by the non-hydrolytic sol–gel method seems more homogeneous than **3** in terms of substructure units (see Table 1). For **5** the quantity was too small for such analysis. For **6**, a qualitative ^{29}Si CP HPDEC spectrum exhibit a broad peak at −62 ppm similar to that found in poly(organosilsesquioxanes). This corroborates the expected formation of [(NCN)$_{1.5}$Si(CH$_2$)$_3$(C$_2$B$_{10}$H$_{10}$)(CH$_2$)$_3$-Si(NCN)$_{1.5}$]$_n$ due to the condensation of the material. Additional signals at 11.4 ppm and 1.7 ppm attributed, respectively, to residual uncondensed CH_2–$SiCl_3$ and C=N–$SiMe_3$ functions are also observed. The compositions of xerogels **3**, **4** and **6** were also estimated by elemental analysis, assuming that the organic groups have not been cleaved during the condensation, and completely condensation. For hydrolytic xerogel **3** the calculated analysis is very consistent with the theoretical, however the non-hydrolytic xerogel **4** gives percentages of C and H which should agree with an uncondensed O(^{i}Pr) group. For xerogel **6**, as a result of the high moisture sensitivity of –NCN groups, different elemental analyses performed from the same sample give distinct results.

Table 1 Degree of condensation for xerogels **3** and **4**

	T^1		T^2		T^3		
Xerogel	ppm	%	ppm	%	ppm	%	LC (%)
3	−49.8	22	−57.4	30	−65.1	48	75
4	−49.4	6	−57.0	63	−66.4	31	75

Meso- and microscopic structure. X-Ray powder diffraction analysis was performed to obtain information about the organization at the micro- and mesoscopic scale. The XRD patterns of xerogels **3** and **4** are similar (Fig. 1), they did not exhibit any sharp Bragg peak, but they present two broad bands consistent with a short-range ordered structure. According to a Bragg's law assumption, these bands correspond to *d* spacings of 15.2 and 6.2 Å for **3**, and 13.8 and 6.2 Å for **4**. The first *d* spacing is associated with the high intensity (001) peak, while 6.2 Å could be associated with the second order (002) peak, for each compound. Additionally, a very smooth broad band at *d* = 3.7 Å (Fig. 1b and d) is also observed. For **6**, the XRD diffraction pattern displays two broad bands close to those found in xerogels **3** and **4**. Additional Bragg's signals indicate the presence of a material with an organisation at a long-rang order, however it is not possible at the present time to decide if it is due to a single compound or a mixture of two different products (Fig. 1c). Thus, all our xerogels exhibit in general a short-range order organization at the nanometre scale when compared to other xerogels that remain completely amorphous,[33] which we have attributed to the presence of the rigid *o*-carborane cluster. In this respect, the signals at 13.8 Å and 15.2 Å are related to the presence of the organo–carborane moiety and the broad shoulder at 3.7 Å is generally attributed to the contribution of the Si–O–Si network.[36] The signal at 13.8 Å is in agreement with a periodic distance due to the organic alkylene bridge, specifically to twice the [C_c–$CH_2CH_2CH_2$–SiO–] fragment, which is estimated to measure 6.85 Å, by computer simulation models of organo–carborane packing within silicate sheets to form a lamellar structure (Fig. 2a). The signal at 6.2 Å could correspond to

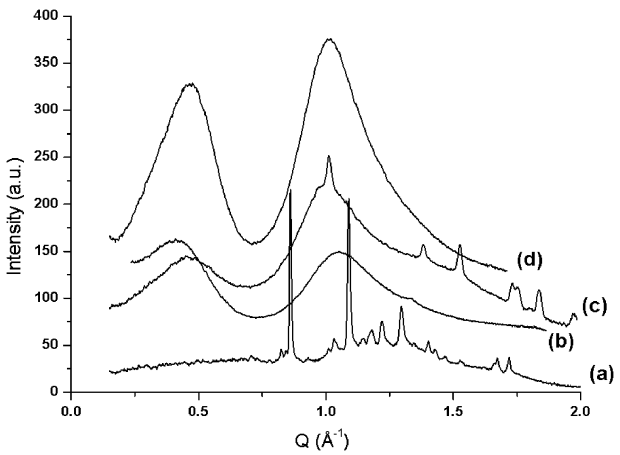

Fig. 1 X-Ray powder diffraction diagrams of: (a) precursor **2**, (b) xerogel **3**, (c) xerogel **6**, (d) xerogel **4**.

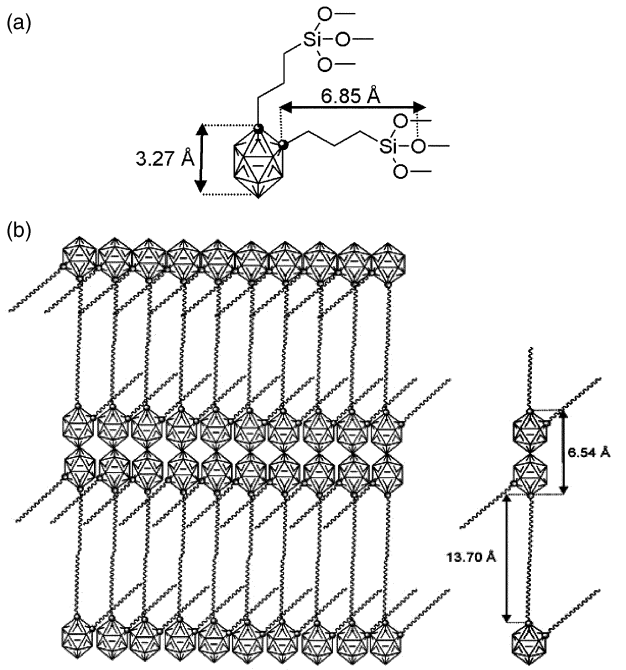

Fig. 2 a) Main distances in the xerogels calculated by computer simulation. b) Proposed organization of the carborane moieties and alkylic chains in xerogels.

a periodic distance of the cluster moiety, since this agrees with twice the distance between the C1 and its antipodes B12 as determined by computer simulation (Fig. 2a), or just to the [C_c–$CH_2CH_2CH_2$–SiO–] fragment. Likewise, this has been interpreted by us as the formation of a periodic structure with alternating organo–carborane and silica layers which represent an unique nanostructuration of the material (Fig. 2b).

For xerogel **5** obtained using the solid-state hydrolytic process by exposing to air the precursor **2**, the XRD diagram shows the same two broad bands as **3**, at 6.1 and 15.1 Å, and two additional sharp peaks at d = 3.4 and 3.3 Å, indicating the presence of a higher level of periodicity (Fig. 3). Compared to the X-ray diffraction powder of the crystallized precursor **2**, there is a difference in the position of the Bragg's peaks of **5**, which exhibits main peaks at 0.86, 1.10, 1.22, 1.30, 1.68, 1.72 $Å^{-1}$ in Q^{-1}. Therefore, although part of the periodical structure is maintained during the solid-state hydrolysis, it is obvious that the initial packing of the precursor is lost and serves as a template leading to the long-range order organization of the xerogel **5** (see Fig. 3).

Transmission electronic microscopy (TEM) studies on the xerogel **4** reveal the great heterogeneity of the materials in terms of organization. Taken from the same sample, a great part of the material appears completely amorphous, while some other parts present a high level of organization. The TEM images presented in Fig. 4 confirm the layered structure of a part of the material in which the interlayer spacing is 3.4 Å. This result might be in agreement with the (004) order with respect to the high intensity (001) peak observed in the XRD pattern. This could be considered as a preliminary result and further studies will be the subject of a future work.

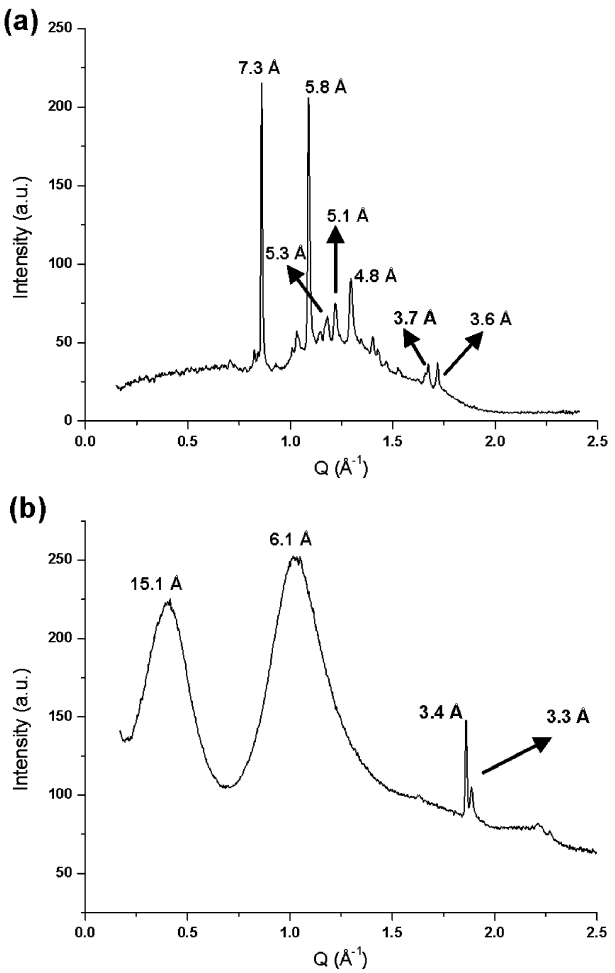

Fig. 3 X-Ray powder diffraction diagrams of: (a) crystallized precursor **2** and (b) xerogel **5**.

Microscopy. Focusing on the hydrolytic solid state condensation of **2**, analysis of the precursor in polarized light agrees with the X-ray data which indicate a crystallised compound highly birefringent and colourful by microscopy. Although part of the colour is lost upon exposure to air, the resulting **5** is still highly birefringent and moreover the shape of the crystalline needles seems to be preserved indicating a very low level of amorphisation during the polycondensation of the crystallised precursor. This is in agreement with the presence of Bragg's signal observed by X-ray diffraction analysis of the material (Fig. 5).

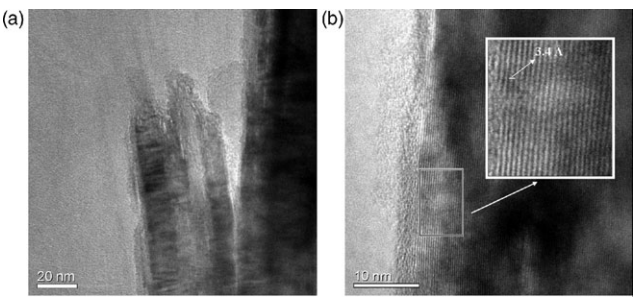

Fig. 4 TEM images for xerogel **4**.

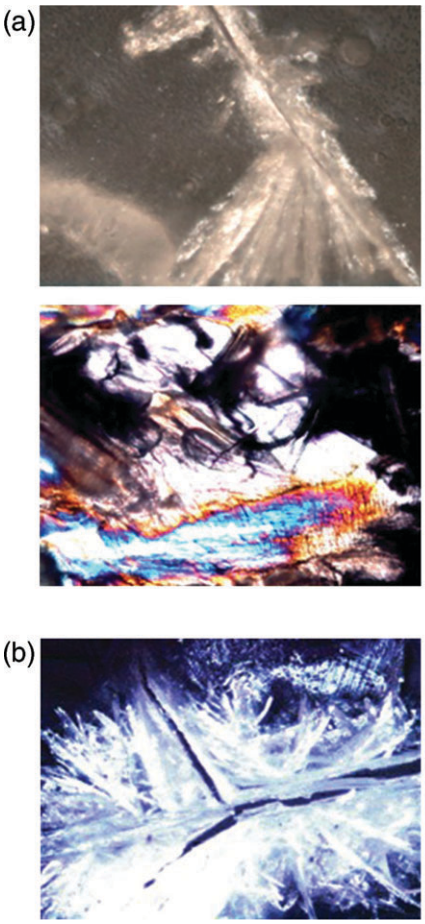

Fig. 5 Optical micrographs in polarized light of: (a) **2** and (b) **5**.

Porosity. The pore structure and the specific surface area of the materials were determined by adsorption/desorption isotherms.[51,52] Xerogels **3** and **4** exhibit very low specific surface areas (<15 m^2 g^{-1}), which could be attributed in a first approach to the presence of the flexible alkyl groups in the material.[37] However, for **6** a much higher specific surface area of 200 m^2 g^{-1} was found by a 5 points porosimetry measurement with BET calculation, which clearly indicates that for the same precursor the type of condensation process and experimental conditions modify the porosity in the gel structure. This may also results from the fact that Si–O–Si bridges are flexible while Si–N═C═N–Si are much more rigid. For **5**, the amount of product was too small for this analysis.

Thermal stability. The thermal behaviour of xerogels studied by thermogravimetric analysis (TGA) in inert argon atmosphere was determined between 20 and 1200 °C at a heating rate of 5 °C min^{-1}, exhibiting high thermal stability. Xerogels **3** and **4** show weight losses between 100 °C and 450 °C, which correspond to 6.1 and 9.6%, respectively, and is attributed to the final condensation of the material (Fig. 6). The main weight loss (around 18%) occurs between 450 and 800 °C, which should correspond to m/z 56, attributed to the loss of two CH_2═CH_2 molecules. Continued heating to temperature

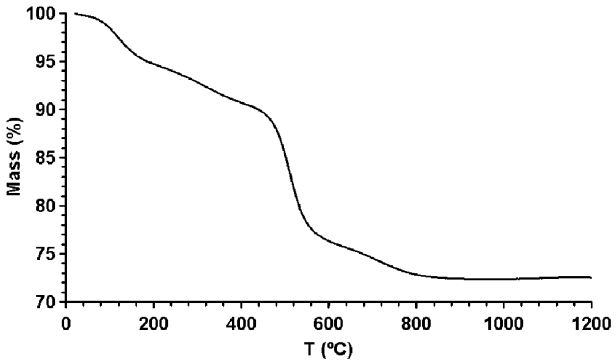

Fig. 6 TGA curve of xerogel **3** under an atmosphere of argon.

of 1200 °C leaves a black residue in 77% yield, whose ATR spectrum exhibits two intense bands at 1370 and 1090 cm^{-1} attributed to ν(B–O) and ν(Si–O), respectively; however no signals corresponding to B–H are observed indicating that the cluster has been completely degraded. In addition, the XRD spectrum of the residue does not exhibit any Bragg's peak, indicating that a completely amorphous material is obtained. In the same conditions, xerogel **6** is stable up to 200 °C, then an 8% weight lost is observed gradually up to 400 °C and could be due to the final condensation of the material, and evaporation of residual bis(trimethylsilyl)carbodiimide.[42] The main weight loss (around 35%) occurs between 400 and 800 °C and is certainly related to the loss of carbon-containing moieties and to the condensation of residual uncondensed groups like $SiCl_3$ and –C═N–$SiMe_3$. In all the cases, elimination of carborane moieties should not be considered since in inert atmosphere *o*-carborane (1,2-$C_2B_{10}H_{12}$) begins to isomerize to *m*-carborane (1,7-$C_2B_{10}H_{12}$) above 425 °C, and above 700 °C the *p*-carborane (1,12-$C_2B_{10}H_{12}$) is obtained.[6]

Conclusions

In the present work we report on the preparation and structural characterization of a new type of carborane-containing class II hybrid material in which the cluster is bonded to the siloxane groups. The key point in the design of such materials has been the introduction of an unusually rigid, chemically and thermally versatile moiety attached through organic spacers to hydrolysable $SiCl_3$ groups ready to condense by different processes. Four hybrid organic–inorganic xerogels (**3–6**) have been prepared using hydrolytic and non-hydrolytic sol–gel polycondensation, the solid-state process and the carbodiimide procedure. Materials prepared by hydrolytic or non-hydrolytic sol–gel methods are very similar in terms of thermal stability, porosity and structure but different in terms of structural T^n subunits. Although a short-range order between the organo–carborane unit can be proposed to describe the structural organisation of these solids, a higher periodicity seems achievable by a solid-state process, in agreement with previous work.[41,53] Finally, the hybrid material **6** prepared from the same precursor exhibits some differences in the porosity, condensation and X-ray structure with respect to

the other materials; all structural characteristics that have to be related to the nature of the Si–N═C═N–Si network. Current work is being carried out to go into the study of the features and behaviour of these and other related materials.

Experimental

Materials

All reactions were carried out under an atmosphere of purified argon using standard Schlenk techniques. Solvents were purified, dried, and distilled by standard procedures. Trichlorosilane and Karstedt platinum catalyst (3–3.5% Pt) were purchased from ABCR. Allyl bromide (99%) and *n*-BuLi were used as received from Aldrich and Lancaster. $FeCl_3$ and pyridine were purchased from Aldrich. $Me_3Si–NCN–SiMe_3$ was prepared according to literature procedures.[42]

Instrumentation

Infrared spectra were measured in NaCl or KBr pellets on a ThermoNicolet AVATAR 320 FT-IR. Attenuated Total Reflection (ATR) spectra were measured on a Bruker Tensor 27 using a Specac NKII Golden Gate accessory. $^1H\{^{11}B\}$ NMR (300.13 MHz), ^{11}B NMR (96.29 MHz), $^{13}C\{^1H\}$ NMR (75.47 MHz) and $^{29}Si\{^1H\}$ NMR (59.62 MHz) spectra were recorded on a Bruker ARX 300 spectrometer. NMR spectra were measured using samples in $CDCl_3$ solution at room temperature. Chemical shifts for ^{11}B NMR were referenced to external $BF_3 \cdot OEt_2$ and those for $^1H\{^{11}B\}$ NMR, $^{13}C\{^1H\}$ NMR and $^{29}Si\{^1H\}$ NMR were referenced to Me_4Si. ^{29}Si CP MAS NMR (at 79.49 MHz) and ^{13}C CP MAS NMR (at 100.63 MHz) spectra were obtained on a Bruker Advance ASX400 using a CP MAS sequence or a HPDEC. Thermogravimetric analyses (TGA) of the network materials were performed on a Netzsch STA 409 PC/PG under a 50 mL min^{-1} argon flow. Samples were heated from 20 to 1200 °C at 5 °C min^{-1}. X-Ray powder diffraction measurements were performed using a spectrometer with a rotating copper anode with an OSMIC monochromator system and an 'Image Plate 2D' detector working with CuKα (λ = 1.542 Å) radiation and a beam size of 0.5 × 0.5 mm and acquisition time of 40 to 50 minutes. Sample were previously crushed and placed in a Lindeman tube (1mm diameter). The specific surfaces areas, porosities, volumes, and pore size distributions were determined by analysing the N_2 adsorption/desorption isotherms according to the BET method using a Micromériticcs Gémini III 2375 and ASAP 2010. TEM images were achieved with a JEOL JEM 2011 (200 Kv) microscope. Elemental analyses were performed in the analytical laboratory using a Flash EA 1112 Series microanalyzer.

Syntheses

1,2-(CH_2–CH═CH_2)$_2$-1,2-$C_2B_{10}H_{10}$ (1). In a Schlenk flask under argon, 1,2-$C_2B_{10}H_{10}$ (1.0095 g, 7.0 mmol) was dissolved in a mixture of toluene (14 ml) and diethyl ether (7 ml). The solution was cooled at 0 °C and *n*-BuLi (9.7 ml, 14.7 mmol) was added dropwise. The mixture was stirred for 1 hour at room temperature, cooled again at 0 °C, and (CH_2═CH–CH_2)Br (1.2 ml, 13.9 mmol) was added. The mixture was stirred for 2 hours at room temperature and refluxed overnight. Then it was cooled to room temperature, and quenched with 20 ml of water, transferred to a separatory funnel and extracted with Et_2O (3 × 10 ml). The organic layer was dried over $MgSO_4$ and concentrated under vacuum to obtain compound **1** (1.51 g, 97%) as a yellow oil. FTIR NaCl/cm^{-1} 3086 ν(═CH_2), 3022 ν(═CH), 2986–2925 ν(C–H)$_{alkyl}$, 1643 ν(C═C) and 1418 δ(═C–H). $^1H\{^{11}B\}$ NMR (δ (ppm)): 2.1 (2H, br s, B–*H*), 2.3 (8H, br s, B–*H*), 2.9 (4H, d, J_1 = 7.3 Hz, C_c–CH_2), 5.1 (2H, d, $J_{1,t}$ = 16.7 Hz, CH═CH_2), 5.2 (2H, d, $J_{1,c}$ = 9.7 Hz, CH═CH_2), 5.8 (2H, m, $J_{1,t}$ = 16.7 Hz, $J_{1,c}$ = 9.7 Hz, J_1 = 7.3 Hz, C*H*═CH_2). ^{11}B NMR (δ (ppm)): −4.5 (2B, d, J_1 = 145.0 Hz), −10.6 (8B, d, J_1 = 153.9 Hz). $^{13}C\{^1H\}$ NMR (δ (ppm)): 132.5 (*C*H═CH_2), 119.5 (CH═*C*H_2), 77.7 (C_c), 39.2 (C_c–*C*H_2).

1,2-[$(CH_2)_3SiCl_3$]$_2$-1,2-$C_2B_{10}H_{10}$ (2). In a Schlenk flask under argon, **1** (950 mg, 4.2 mmol), $HSiCl_3$ (1.71 ml, 16.9 mmol) and Karstedt catalyst (16 µl, 0.034 mmol) were mixed and stirred for 2 hours at room temperature. Evaporation of the volatiles and the excess of $HSiCl_3$ gave compound **2** (2.10 g, ≈99%) as yellow oil. $^1H\{^{11}B\}$ NMR (δ (ppm)): 1.46 (4H, t, J_1 = 8.1 Hz, –CH_2–Si), 1.86 (4H, m, –CH_2–CH_2–Si), 2.29 (4H, t, J_1 = 8.1 Hz, B–C_c–CH_2–). ^{11}B NMR (δ (ppm)): −3.6 (2B, d, J_1 = 141.4 Hz), −9.4 (8B, m). $^{13}C\{^1H\}$ NMR (δ (ppm)): 78.5 (C_c), 36.4 (C_c–*C*H_2), 23.7 (*C*H_2–CH_2), 22.6 (*C*H_2–Si). $^{29}Si\{^1H\}$ NMR (δ (ppm)): 11.6.

Hydrolytic xerogel 3. In a Schlenk flask under argon, **2** (792 mg, 1.6 mmol) was dissolved in THF (2 ml). After all the precursor was dissolved, H_2O (0.2 ml, 9.9 mmol) was added dropwise to the solution. Once the addition was completed, a white solid was observed and the suspension was stirred for 30 minutes. The stirring was then stopped to allow gelation. After 5 minutes a gel was formed and was kept for 1 week for aging. The solid and the liquid phases were separated by filtration. The isolated gel was crushed and washed with ethanol (3 × 10 ml), acetone (3 × 10 ml) and diethyl ether (3 × 10 ml), and finally dried under vacuum to obtain xerogel **3** (279 mg, 53%). FTIR KBr/cm^{-1} 2958–2888 ν(C–H)$_{alkyl}$, 2594 ν(B–H), 1458 δ(C–H)$_{alkyl}$, 1196 δ(Si–CH), 1078 ν(Si–O–Si). ^{29}Si NMR CP-MAS (δ (ppm)): −49 (T^1), −56 (T^2), −65 (T^3). ^{13}C CP MAS NMR (δ (ppm)): 80 (C_c), 37 (C_c–*C*H_2), 24 (*C*H_2–CH_2), 14 (*C*H_2–Si). X-Ray powder diffraction shows two broad bands with *d* spacings of 6.2 Å and 15.2 Å. The surface area measure using the N_2 BET technique is 13 m^2 g^{-1}. Anal. Calc. for $C_8H_{22}B_{10}Si_2O_3$: C, 29.1; H, 6.7%. Found: C, 28.9; H, 6.6%.

Non-hydrolytic xerogel 4. In a Schlenk flask under argon, **2** (730 mg, 1.5 mmol) was dissolved in $^iPr_2O$ (0.63 ml) and $FeCl_3$ (0.1%) catalyst was added to the solution. The mixture was stirred for 5 minutes and transferred under N_2 to another tube, which was frozen in liquid nitrogen and sealed under vacuum. The sealed tube was held at 110 °C in an oven for 43 hours and then opened under argon. The obtained gel was crushed and washed with ethanol (3 × 10 ml), acetone (3 × 10 ml) and diethyl ether (3 × 10 ml), and finally dried under vacuum to obtain xerogel **4** (352 mg, 72%). FTIR KBr/cm^{-1} 2950–2880 ν(C–H)$_{alkyl}$, 2592 ν(B–H), 1458 δ(C–H)$_{alkyl}$, 1196 δ(Si–CH),

1063 ν(Si–O–Si). ^{29}Si CP MAS NMR (δ (ppm)): −49 (T^1), −56 (T^2), −65 (T^3). ^{13}C CP MAS NMR (δ (ppm)): 80 (C_c), 37 (C_c–CH_2), 24 (CH_2–CH_2), 14 (CH_2–Si). X-Ray powder diffraction shows two broad bands with *d* spacings of 6.2 Å and 13.8 Å. The surface area measure using the N_2 BET technique is 8 m^2 g^{-1}. Anal. Calc. for $C_8H_{22}B_{10}Si_2O_3$: C, 29.1; H, 6.7%. Found: C, 32.6; H, 7.6%.

Solid-state hydrolytic xerogel 5. Some drops of a solution of **2** in CH_2Cl_2 were deposited on a microscope slide under argon until the formation of some crystals was observed. Then pictures of these crystals were taken using an electronic microscope. After this, the crystals were exposed to air for 19 days to form a white gel, which was insoluble in CH_2Cl_2. Again, some pictures of the solid were taken. FTIR KBr/cm^{-1} 2950–2880 ν(C–H)$_{alkyl}$, 2594 ν(B–H), 1458 δ(C–H)$_{alkyl}$, 1196 δ(Si–CH), 1078 ν(Si–O–Si). X-Ray powder diffraction shows two broad bans with *d* spacings of 6.1 Å, 15.1 Å, 3.4 Å and 3.3 Å.

Silsesquicarbodiimide xerogel 6. In a Schlenk flask under argon, **2** (693 mg, 1.4 mmol) was dissolved in THF (3 ml). Then, Me_3Si–NCN–$SiMe_3$ (0.97 ml, 4.2 mmol) and pyridine (0.06 ml, 0.7 mmol) were added to the solution and stirred at room temperature for 1 hour. After this time, a white gel was obtained and allowed to age for 1 week at 45 °C. The gel was crushed, treated with dry THF (10 ml), filtered and washed with dry THF (2 × 10 ml) under argon. Finally, the solid was dried under vacuum at 130 °C for a day to obtain xerogel **6** (571 mg, 80%). FTIR KBr/cm^{-1} 2950–2880 ν(C–H)$_{alkyl}$, 2592 ν(B–H), 2152 ν(Si–NCN), 1459 δ(C–H)$_{alkyl}$, 1254 δ(Si–CH_2). ^{29}Si CP MAS NMR (δ (ppm)): 11.4, 1.7, −62. ^{13}C CP MAS NMR (δ (ppm)): 121 (NCN), 80 (C_c), 38 (C_c–CH_2), 24 (CH_2–CH_2), 18 (CH_2–Si). X-Ray powder diffraction shows two broad bands with *d* spacings of 5.9 Å and 13.7 Å, and additional Bragg's peaks with *d* spacings of 4.3, 3.8, 3.4, 3.3 and 3.2 Å. The surface area measure using the N_2 BET technique is 200 m^2 g^{-1}.

Acknowledgements

This work was supported by MCyT, MAT2004-01108 and Generalitat de Catalunya, 2001/SGR/00337. A. G. thanks MCyT for a FPI grant annexed to MAT01-1575.

References

1 R. B. King, *Chem. Rev.*, 2001, **101**, 1119.
2 M. F. Hawthorne, *Advances in Boron Chemistry*, The Royal Society of Chemistry, Cambridge, UK, 1997, p. 261.
3 M. F. Hawthorne, in *Current Topics in the Chemistry of Boron*, ed. G. W. Kabalka, The Royal Society of Chemistry, Cambridge, UK, 1994, p. 207.
4 R. N. Grimes, *Carboranes*, Academic Press, New York, 1970, p. 54.
5 V. I. Bregadze, *Chem. Rev.*, 1992, **92**, 209.
6 J. Plesek, *Chem. Rev.*, 1992, **92**, 269.
7 R. Hamasaki, M. Ito, M. Lamrani, M. Mitsuishi, T. Miyashita and Y. Yamamoto, *J. Mater. Chem.*, 2003, **13**, 21.
8 J. T. Taylor, J. Carusso, A. Newlon, U. Englich, K. Ruhlandt-Sende and J. T. Spencer, *Inorg. Chem.*, 2001, **40**, 3381.
9 M. Lamrani, R. Hamasaki, M. Mitsuishi, T. Miyashita and Y. Yamamoto, *Chem. Commun.*, 2000, 1595.
10 P. Kaszynski and D. Lipiak, in *Materials for Optical Limiting*, ed. R. Crane, K. Lewis, E. V. Stryland and M. Khoshnevisan, MRS, USA, 1995, vol. 374, p. 341.
11 K. Ohta, A. Januszko, P. Kaszynski, T. Nagamine, G. Sasnouski and Y. Endo, *Liq. Cryst.*, 2004, **31**, 671.
12 A. G. Douglass, K. Czuprynski, M. Mierzwa and P. Kaszynski, *Chem. Mater.*, 1998, **10**, 2399.
13 P. Kaszynski, S. Pakhomov and K. F. Tesh, *Inorg. Chem.*, 2001, **40**, 6622.
14 W. Piecek, J. M. Kaufman and P. Kaszynsky, *Liq. Cryst.*, 2003, **30**, 39.
15 M. Ichitani, K. Yonezawa, K. Okada and T. Sugimoto, *Polym. J.*, 1999, **31**, 908.
16 S. Papetti, B. B. Schaeffer, A. P. Gray and T. L. Heying, *J. Polym. Sci., Polym. Chem. Ed.*, 1966, **4**, 1623.
17 (*a*) E. J. Houser and T. M. Keller, *J. Polym. Sci., Part A: Polym. Chem.*, 1998, **36**, 1969; (*b*) E. J. Houser and T. M. Keller, *Macromolecules*, 1998, **31**, 4038; (*c*) *High Temperature Siloxane Elastomers*, ed. P. R. Dvornic and R. W. Lenz, Hutthing & Wepf Verlag, Basel, Heidelberg, New York, 1990.
18 H. Kimura, K. Okita, M. Ichitani, T. Sugimoto, S. Kuroki and I. Ando, *Chem. Mater.*, 2003, **15**, 355.
19 T. K. Dougherty, *US Pat.*, 235,264,285, 1993.
20 M. F. Hawthorne, in *Advance in Boron and the Boranes*, ed. J. F. Liebman, A. Grenberg and R. S. Williams, VCH, New York, 1988, p. 225.
21 F. Teixidor, M. A. Flores, C. Viñas, R. Kivekäs and R. Sillanpää, *Angew. Chem., Int. Ed. Engl.*, 1996, **108**, 2388.
22 F. Teixidor, M. A. Flores, C. Viñas, R. Sillanpää and R. Kivekäs, *J. Am. Chem. Soc.*, 2000, **122**, 1963.
23 O. Tutusaus, S. Delfosse, A. Demonceau, A. F. Noël, C. Viñas, R. Núñez and F. Teixidor, *Tetrahedron Lett.*, 2002, **43**, 983.
24 Z. Xie, *Acc. Chem. Res.*, 2003, **36**, 1.
25 O. Tutusaus, C. Viñas, R. Núñez, F. Teixidor, A. Demonceau, S. Delfosse, A. F. Noël, I. Mata and E. Molins, *J. Am. Chem. Soc.*, 2003, **125**, 11830.
26 P. E. Benken, D. C. Busby, M. S. Delany, R. E. King, C. W. Kreimendahl, T. B. Marder, J. J. Wilczynski and M. F. Hawthorne, *J. Am. Chem. Soc.*, 1984, **106**, 7444 and references therein.
27 M. F. Hawthorne and A. Maderna, *Chem. Rev.*, 1999, **99**, 3421.
28 K. J. Winberg, G. Barberà, L. Eriksson, F. Teixidor, V. Tomalchev, C. Viñas and S. Sjöberg, *J. Organomet. Chem.*, 2003, **680**, 188.
29 C. Masalles, J. Llop, C. Viñas and F. Teixidor, *Adv. Mater.*, 2002, **14**, 826.
30 C. Viñas, S. Gomez, J. Bertran, F. Teixidor, J.-F. Dozol and H. Rouquette, *Inorg. Chem.*, 1998, **37**, 3640.
31 B. Grüner, J. Plesek, J. Baca, I. Cisarova, J.-F. Dozol, H. Rouquette, C. Viñas, P. Selucky and J. Rais, *New J. Chem.*, 2002, **26**, 1519.
32 C. Viñas, S. Gomez, J. Bertran, F. Teixidor, J.-F. Dozol and H. Rouquette, *Chem. Commun.*, 1998, 191.
33 K. J. Shea, J. Moreau, D. A. Loy, R. J. P. Corriu and B. Boury, *Functional Hybrid Materials*, ed. C. Sánchez and P. Gómez-Romero, Viley-VCH, Weinheim, 2004, p. 50.
34 D. Avnir, *Acc. Chem. Res.*, 1995, **28**, 328.
35 R. J. P. Corriu and D. Leclercq, *Angew. Chem., Int. Ed. Engl.*, 1996, **35**, 4001.
36 B. Boury and R. J. P. Corriu, *Chem. Rec.*, 2003, **3**, 120.
37 D. A. Loy and K. Shea, *Chem. Rev.*, 1995, **95**, 1431.
38 Z.-L. Lu, E. Lindner and A. Hermann, *Chem. Rev.*, 2002, **102**, 3543.
39 B. Boury and R. J. P. Corriu, *Chem. Commun.*, 2002, 795.
40 S. W. Carr, M. Motavelli, D. Li Ou and A. C. Sullivan, *J. Mater. Chem.*, 1997, **7**, 865.
41 B. Boury, F. Ben and R. J. P. Corriu, *Angew. Chem., Int. Ed.*, 2001, **40**, 2853.
42 A. O. Gabriel, R. Riedel and W. F. Maier, *Appl. Organomet. Chem.*, 1997, **11**, 833.
43 S. Nahar-Borchert, E. Kroke, R. Riedel, B. Boury and R. J. P. Corriu, *J. Organomet. Chem.*, 2003, **686**, 127.
44 A. O. Gabriel and R. Riedel, *Angew. Chem., Int. Ed. Engl.*, 1997, **36**, 384.
45 A. N. Kashin, K. P. Butin, V. I. Stanko and I. P. I. Beletskaya, *Izv. Akad. Nauk. SSSR, Ser. Khim.*, 1969, **9**, 1917.

46 J. F. Valliant, A. S. King, P. Morel, P. Schaffer, O. O. Sogbein and K. A. Stephenson, *Coord. Chem. Rev.*, 2002, **232**, 173.
47 L. Bourget, R. J. P. Corriu, D. Leclercq, P. H. Mutin and A. Vioux, *J. Non-Cryst. Solids*, 1998, **242**, 81.
48 L. Bourget, P. H. Mutin, A. Vioux and J. M. Frances, *J. Polym. Sci., Part A: Polym. Chem.*, 1998, **36**, 2415.
49 *Silicon in Organic Organometallic and Polymer Chemistry*, ed. M. A. Brook, John Wiley & Sons Inc., New York, 1999.
50 G. Cervau, R. J. P. Corriu, C. Lepeytre and H. P. Mutin, *J. Mater. Chem.*, 1998, **8**, 2707.
51 *Powder Surface and Porosity*, ed. S. Lowell and J. E. Shields, Chapman and Hall, London, 1984.
52 S. J. Gregg and S. W. Sing, *Adsorption, Surface Area and Porosity*, Academic Press, London, 1982.
53 N. Liu, K. Yu, B. Smarsly, D. R. Dunphy, Y.-B. Jiang and C. J. Brinker, *J. Am. Chem. Soc.*, 2002, **124**, 14540.